Article

Discovery Medicine 2024; 36(183): 816–826
https://doi.org/10.24976/Discov.Med.202436183.76

TRIM27-Induced Protective Autophagy: A Novel Therapeutic Approach for Pneumonia

Yajiao Pang[1], Hongrong Wang[1], Qiaoyi Xie[1], Tingting Ma[2,*]

[1]Department of Pediatrics, The Affiliated People's Hospital of Ningbo University, 315000 Ningbo, Zhejiang, China
[2]Department of Infectious Diseases, Ningbo Yinzhou No.2 Hospital, 315000 Ningbo, Zhejiang, China
*Correspondence: nbmatingting1129@163.com (Tingting Ma)
Published: 20 April 2024

Background: Pneumonia is a prevalent respiratory ailment involving complex physiological and pathological mechanisms. The tripartite motif containing 27 (TRIM27) plays a crucial role in regulating inflammation mechanisms. Therefore, the purpose of this study is to further explore the therapeutic potential of TRIM27 in pneumonia, based on its regulatory mechanisms in inflammation and autophagy.

Methods: This study established a mouse pneumonia animal model through lipopolysaccharide (LPS) administration, designating it as the LPS model group. Subsequently, adenovirus-mediated TRIM27 overexpression was implemented in the animals of the LPS model group, creating the TRIM27 treatment group. After a 7-day treatment period, lung tissues from the mice were collected. Various techniques, including immunohistochemistry, quantitative reverse transcription PCR (RT-qPCR), western blot, enzyme-linked immunosorbent assay (ELISA), and electron microscopy were utilized to analyze the impact of TRIM27 overexpression on inflammatory factors, oxidative stress, autophagy, and inflammatory processes in pulmonary tissues. Finally, an *in vitro* LPS cell model was established, and the effects of TRIM27 overexpression and autophagy inhibition on inflammatory cytokines and autophagosomes in LPS-induced inflammatory cells were examined through RT-qPCR and immunofluorescence techniques.

Results: The research findings demonstrate a significant reduction in the elevated levels of interleukin-6 (IL-6), IL-1β, and Tumor necrosis factor-alpha (TNF-α) induced by LPS with TRIM27 overexpression ($p < 0.01$). Conversely, the autophagy inhibitor 3-Methyladenine (3-MA) diminished the effects induced by TRIM27 overexpression. Moreover, TRIM27 overexpression enhanced the expression of Microtubule-associated protein 1A/1B light chain 3 (LC3) II/I and Beclin-1 proteins in mice subjected to LPS stimulation ($p < 0.01$), while reducing the expression of the p62 protein ($p < 0.01$). The addition of 3-MA, however, decreased Beclin-1 expression and inhibited autophagy ($p < 0.01$). Additionally, TRIM27 overexpression decreased the expression of NOD-like receptor thermal protein domain associated protein 3 (*NLRP3*), cleaved caspase-1, *IL-1*β, and Gasdermin D N-terminal fragment (GSDMD-N) proteins in LPS-stimulated mice ($p < 0.05$). TRIM27 overexpression also decreased the levels of malondialdehyde (MDA), Activating Transcription Factor 6 (*ATF6*), and C/EBP-homologous protein (*CHOP*), while increasing the levels of superoxide dismutase (SOD) and glutathione (GSH) in mice exposed to LPS ($p < 0.01$).

Conclusion: The induction of TRIM27 overexpression emerges as a potential and effective pneumonia treatment. The underlying mechanism may involve inducing protective autophagy, thereby reducing oxidative stress and cell pyroptosis.

Keywords: TRIM27; autophagy; pneumonia; inflammation; oxidative stress; ER stress

Introduction

Pneumonia is a prevalent respiratory ailment characterized by inflammation, oxidative stress, and endoplasmic reticulum (ER) stress [1]. Pneumonia is a high-prevalence and high-mortality disease globally [2]. The pathogenesis of pneumonia involves complex interactions between host immune responses and microbial elements [3,4]. A comprehensive understanding of the underlying mechanisms is crucial to identifying potential therapeutic targets and developing effective interventions [5,6].

Autophagy is a crucial cellular mechanism that involves the breakdown and reuse of impaired organelles and proteins [7,8]. Under stressful conditions, this highly regulated process maintains cellular homeostasis and promotes cell survival [9]. Autophagy has demonstrated its importance in eliminating intracellular pathogens and regulating inflammatory reactions [10]. Dysregulation of autophagy has been associated with the onset of various illnesses, such as infectious and inflammatory diseases [11,12]. In recent years, increasing evidence suggests a reciprocal interaction between autophagy and inflammation [13]. Autophagy possesses the ability to modulate the production of pro-inflammatory cytokines and regulate the activation of inflammatory signaling pathways [14]. Conversely, inflammation can regulate autophagy, promoting or inhibit-

ing its activity depending on the circumstances [15]. Hence, the interaction between autophagy and inflammation plays a crucial role in the onset and progression of illnesses [16].

The tripartite motif containing 27 (TRIM27), also known as Red Fluorescent Protein (RFP), belongs to the TRIM protein family characterized by the tripartite motif [17]. TRIM27 is involved in multiple cellular processes, including innate immunity, inflammation, and autophagy [18]. Recent studies highlight the role of TRIM27 in controlling immune responses and maintaining cellular homeostasis [19,20]. However, its specific role in pneumonia is not completely understood.

The protective function of induced autophagy in pneumonia is supported by molecular mechanisms that include the control of autophagy-associated genes, modulation of autophagy pathway signaling, elimination of impaired organelles and proteins, and regulation of inflammatory responses and immune reactions [21]. By regulating these mechanisms, it is possible to mitigate cellular harm and inflammatory reactions resulting from pneumonia, thus safeguarding the lungs against additional harm [22]. During pneumonia, the regulation of autophagy-related genes like Beclin-1, Autophagy-related protein 5 (ATG5), and Microtubule-associated protein 1A/1B light chain 3 (LC3) may occur [23]. Alterations in the levels of the autophagy-associated genes can influence the development and severity of pneumonia. This study investigated the impact of TRIM27 on pneumonia and its influence on autophagy. The protective effect of TRIM27-induced autophagy was assessed using a mouse model and cell experiments by measuring cytokine levels, autophagy protein levels, and autophagosome formation.

The findings from this study offer a significant theoretical foundation for further investigation into the utilization of TRIM27 in managing and preventing pneumonia. Furthermore, the discovery that the autophagy suppressor 3-Methyladenine (3-MA) can counteract the inhibitory impact of TRIM27 on autophagy indicates that the regulation of autophagy may be a crucial mechanism underlying the protective influence of TRIM27. Further investigation will contribute to the clarification of the mechanisms through which TRIM27 affects pneumonia and provide new perspectives for the advancement of innovative treatment approaches.

Methods

Lipopolysaccharide (LPS)-Induced Pneumonia Animal Model and Adeno-Associated Virus (AAV)-Mediated Overexpression of TRIM27

Thirty male C57BL/6J mice (30 ± 2 g) were acquired from Beijing Vital River Laboratory Animal Technology Co., Ltd. at around 8 weeks old. The mice were housed in a specific-pathogen-free (SPF) facility that maintained a temperature of 23 ± 1 °C and a 12-hour light-dark cycle. Using a random number table method, 30 mice were randomly divided into three groups (control group, LPS+OE-NC group, and LPS+TRIM27 group). Mice in the LPS+OE-NC group were anesthetized with pentobarbital sodium (50 mg/kg) and secured on a clean surgical table. After shaving and disinfecting the skin around the neck, a midline incision was made to expose the trachea. Subsequently, 2 mg/kg LPS (HY-D1056, MedChemExpress, Monmouth Junction, NJ, USA) dissolved in physiological saline at a concentration of 2 g/L was injected slowly using a 1 mL syringe. After injection, the syringe was immediately removed, and the animals were held upright for 5 seconds to facilitate the distribution of the drug in the lungs. The incision was then sutured. Based on the LPS model group, negative control adenovirus (10^9 pFU/0.1 mL) was injected into the trachea using a bent needle to establish the LPS+OE-NC treatment group. Using the same technique, an equivalent volume of physiological saline was injected into the trachea in the control group. The successful induction of the pneumonia model was validated by monitoring an increase in the respiratory rate of mice. Based on the LPS model group, TRIM27 overexpression adenovirus (10^9 pFU/0.1 mL) was injected into the trachea using a bent needle to establish the TRIM27 overexpression group. The promoter used for TRIM27 overexpression was the Cytomegalovirus Promoter. Mice were euthanized via pentobarbital sodium injection (100 mg/kg). All procedures were approved by the Animal Ethics Committee of Ningbo University (NO.11679).

Histological Analysis

After administering a lethal dose of anesthesia, the thoracic cavity was promptly incised to extract the pulmonary tissue. The extracted lung tissue was separated into two sections, with one section being stored at –80 °C and the other preserved in a 4% paraformaldehyde buffer. The lung tissue that had been fixed for 24 hours was then placed in paraffin for embedding. Sections of 5 µm thickness were obtained from the paraffin-embedded lung tissue using a microtome. These sections were then deparaffinized and rehydrated. Alterations in morphology were noted following the standard staining procedure with hematoxylin and eosin (H&E) (G1120, Solarbio, Beijing, China), and analysis was conducted using the ImagePro Plus software (Version 6.1, Media Cybernetics, Rockville, MD, USA).

Injury Caused by LPS in Cell Cultures

Mice pulmonary epithelial cells (TC-1 cells) (iCell-m080, Beyotime, Shanghai, China) were cultured in Dulbecco's Modified Eagle Medium (DMEM) (iCell-138-0001, Cellverse Bioscience Technology Co., Ltd., Shanghai, China) supplemented with 10% heat-treated fetal bovine serum at 37 °C in a humid environment with 5% CO_2. The cells underwent various interventions (control group, LPS+OE-NC group, LPS+TRIM27 group, LPS+TRIM27+3-MA group). In the LPS group, cells were

Table 1. The primers and their sequences.

Primes name	Primes sequences
IL-6-F	5′-GGCCTTCCCTACTTCACAAG-3′
IL-6-R	5′-ATTTCCACGATTTCCCAGAG-3′
IL-1β-F	5′-ATGGCAACTGTTCCTGAACTCAACT-3′
IL-1β-R	5′-CAGCTCATATGGGTCCGACAG-3′
TNF-α-F	5′-AGCCCCCAGTCTGTATCCTT-3′
TNF-α-R	5′-AGTTGAGATCCATGCCGTTG-3′
ATF6-F	5′-ATGGCTGACCTTTGCCTGAACT-3′
ATF6-R	5′-TCACGGCCCTCTTTCACCTC-3′
CHOP-F	5′-ATGGCAGCTGAGTCTGGAAC-3′
CHOP-R	5′-TCAGCCGTTTCCTGAGGTT-3′
Beclin-1-F	5′-ATGGATGAGATGAGTATGAGC-3′
Beclin-1-R	5′-TCAGCCGTTTCCTGAGGTT-3′
GAPDH-F	5′-ATGGTGAAGGTCGGTGTGAAC-3′
GAPDH-R	5′-TCATGAGCCCTTCCACAATG-3′

IL-6, interleukin-6; *TNF*-α, Tumor necrosis factor-alpha; *ATF6*, Activating Transcription Factor 6; *CHOP*, C/EBP-homologous protein; GAPDH, Glyceraldehyde 3-Phosphate Dehydrogenase; F, forward sequence; R, reverse sequence.

provoked with 10 milligrams per liter of LPS for 24 hours to establish an *in vitro* cellular model. In the LPS+TRIM27 group, cells were subjected to TRIM27 overexpression adenovirus intervention therapy based on the LPS model group. Based on the LPS+TRIM27 treatment group, the LPS+TRIM27+3-MA group cells were treated with the autophagy inhibitor 3-MA (2 mM) (HY-19312, MedChemExpress, Monmouth Junction, NJ, USA). The cell lines utilized in this study underwent mycoplasma detection testing. All the cells involved in this study had completed mycoplasma detection and STR identification.

Quantitative Reverse Transcription PCR (RT-qPCR) Detection of mRNA

After euthanizing the mice, tissue samples were obtained and mRNA levels were measured using qPCR. TRIzol (15596026, Thermo Fisher Scientific, Wilmington, Massachusetts, USA) was used to extract total mRNA, which underwent reverse transcription using PrimeScript-RT (RR037A, Takara Bio, Tokyo, Japan). The resulting cDNA was amplified using the SYBR Premix Ex Taq kit (RR390A, Takara Bio, Tokyo, Japan), and the RT-qPCR conditions were set at 37 °C for 15 minutes for reverse transcription, followed by 5 seconds at 85 °C, and 5 minutes at 95 °C. Subsequently, 40 cycles of amplification were performed at 95 °C for 30 seconds and 65 °C for 45 seconds. Glyceraldehyde 3-Phosphate Dehydrogenase (GAPDH) was used as the internal reference. The relative mRNA expression levels were analyzed using the $2^{-\Delta\Delta Ct}$ method. The primers and their sequences used in this study are listed in Table 1.

Western Blot

Quantification of protein content was conducted using the Bicinchoninic Acid (BCA) assay kit (E112-01, Vazyme, Nanjing, China). For electrophoresis, 30 µg of total protein was loaded onto a 10% polyacrylamide gel, applying a voltage of 80–120 V for 90 minutes. Wet transfer was performed onto a Polyvinylidene Fluoride (PVDF) membrane at a constant voltage of 100 mV. The membrane was then placed in a solution of 5% bovine serum albumin and left at room temperature for 1 hour. The separated proteins were incubated overnight at 4 °C with primary antibodies against LC3 (1:1000; cat no, M186-3; MBL, Kawasaki, Kanagawa Prefecture, Japan), p62 (1:1000; cat no, ab207305; Abcam, Cambridge, UK), Beclin-1 (1:1000; cat no, ab302669; Abcam, Cambridge, UK), NOD-like receptor thermal protein domain associated protein 3 (NLRP3) (1:1000; cat no, ab263899; Abcam, Cambridge, UK), cleaved-caspase-1 (1:1000; cat no, ab32042; Abcam, Cambridge, UK), cleaved interleukin-1β (IL-1β) (1:1000; cat no, Asp116; Cell signaling technology), Gasdermin D N-terminal fragment (GSDMD-N) (1:1000; cat no, ab215203; Abcam, Cambridge, UK), and GAPDH (1:1000; cat no, ab8245; Abcam, Cambridge, UK). Afterward, the proteins were washed and incubated with secondary antibodies (1:2000; cat no, ZB-2305, ZB-2301; ZSGB-BIO, Beijing, China) at room temperature for 1 hour. Finally, proteins were quantified using a chemiluminescence enhancement kit (E-IR-R300, Elabscience Biotechnology Co., Ltd., Wuhan, China). GAPDH served as the internal reference. ImageJ software (Version 1.5f, National Institutes of Health, MD, USA) was used to analyze the grayscale values of the target bands.

Detection of SOD, MDA, and GSH Levels

After homogenizing the frozen lung tissue, the supernatant was obtained through RIPA lysis. Superoxide dismutase (SOD) (A001-3-2), malondialdehyde (MDA) (A003-1-2), and glutathione (GSH) (A006-2-1) assay kits were purchased from Nanjing Jiancheng Bioengineering Institute (Nanjing, China). The diluted antibodies were introduced into every reaction well (100 µL of buffer) in accordance with the guidelines provided by the enzyme-linked immunosorbent assay (ELISA) kit. After incubation overnight at 4 °C, and the plate was washed three times the following day. The samples were then added to the coated reaction wells and incubated at 37 °C for an hour. After washing the plate, enzyme-labeled antibodies were introduced and left to incubate at 37 °C for 1 hour. The TMB substrate solution was introduced and incubated at 37 °C for 30 minutes. After stopping the reaction, the optical density (OD) was measured at 450 nm utilizing an ELISA reader (Cmax plus, Molecular Devices Corporation, Silicon Valley, CA, USA). The concentrations of each substance in the samples were calculated based on the standard curve.

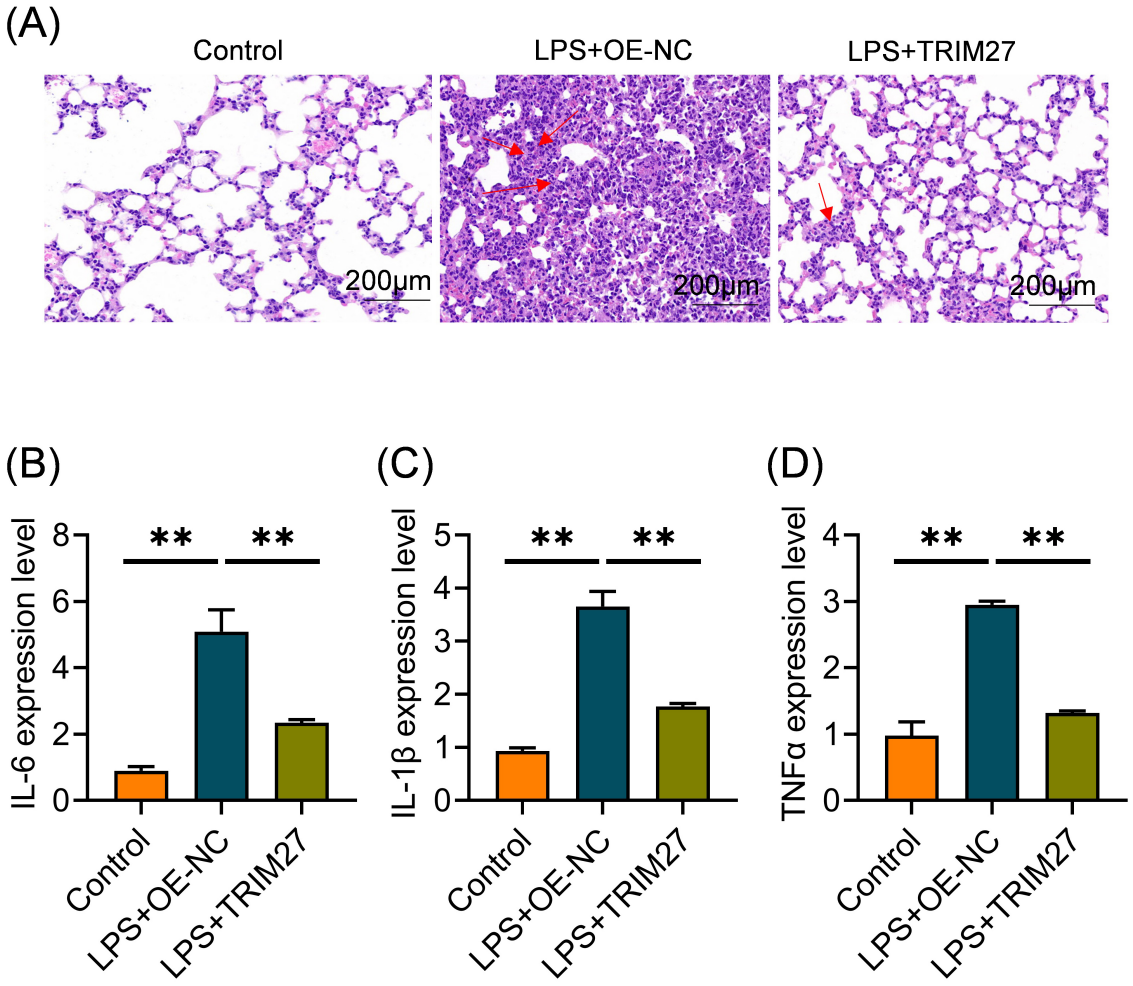

Fig. 1. Tripartite motif containing 27 (TRIM27) alleviates lung tissue damage. (A) Histological examination of lung samples obtained from control mice, lipopolysaccharide (LPS)-exposed mice, and LPS-treated mice with TRIM27. The red arrow represents the area of inflammatory cell infiltration. (B–D) The levels of *IL-6* (B), *IL-1β* (C), and *TNF-α* (D). mRNA in mice lung tissues was measured by quantitative reverse transcription PCR (RT-qPCR) (n = 10). $^{**}p < 0.01$.

Immunofluorescence Detection of Autophagosomes

A population of cells in the logarithmic growth stage were seeded into each well at a density of 1×10^4 cells. After achieving 70% confluence, the cells underwent serum deprivation for 24 hours in a serum-free medium. Following three washes with PBS, the cells were treated with 4% paraformaldehyde for 30 minutes. Permeabilization was achieved with Triton X-100 for 20 minutes, and the cells were then blocked with 5% BSA at room temperature for 60 minutes. The LC3B primary antibody (1:1000; cat no, ab63817; Abcam, Cambridge, UK) was added and incubated at 4 °C overnight, followed by three PBS washes. The fluorescent secondary antibody (1:1000; cat no, A-11008; Invitrogen, Carlsbad, CA, USA) was introduced and left to incubate for 1 hour at room temperature. Following the PBS wash, the cells were subsequently stained with DAPI (C0060, Solarbio, Beijing, China). The examination was conducted using a microscope (CX23, Olympus, Tokyo, Japan).

Statistical Analysis

The statistical analysis was conducted utilizing SPSS 22.0 software (IBM, Armonk, NY, USA). The measurement data is displayed as the mean plus the standard error of the mean (Mean ± Standard Error of the Mean (SEM)). Multiple comparisons between groups were conducted using one-way analysis of variance (ANOVA), while pairwise comparisons were performed using the LSD-*t* test. Statistical significance was established at p-value < 0.05.

Results

TRIM27 Alleviates Lung Tissue Damage

The involvement of TRIM27 in childhood pneumonia was investigated using a mouse model that induced lung inflammation through lipopolysaccharide (LPS) exposure. The mice were categorized into three groups: the control group, the LPS group, and the LPS+TRIM27 group. Histological examination was conducted on lung tissues to mea-

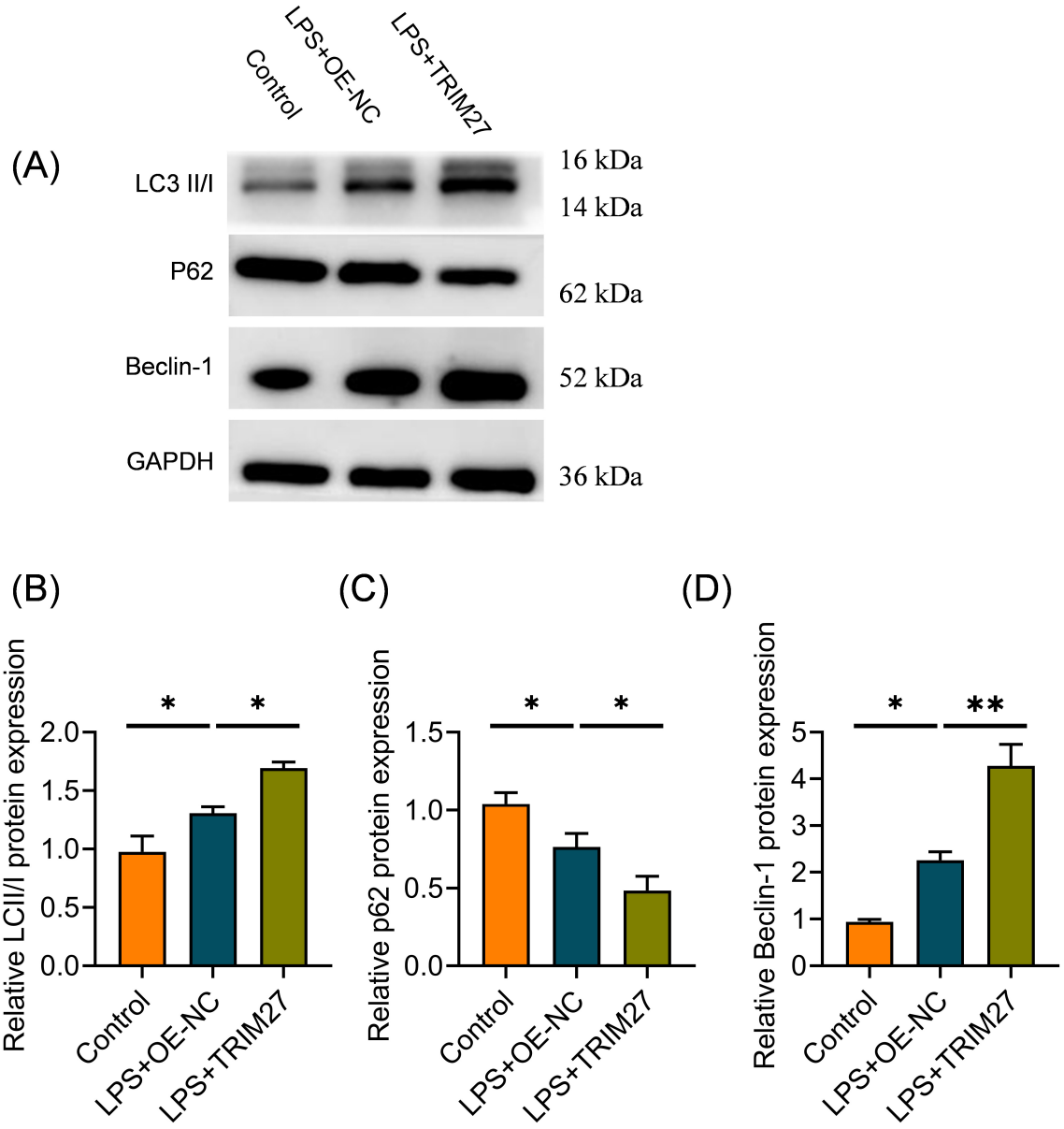

Fig. 2. TRIM27 induces autophagy in LPS-stimulated mice *in vivo*. (A–D) The groups were assessed for the levels of Microtubule-associated protein 1A/1B light chain 3 (LC3) II/I, p62, and Beclin-1 by western blot (n = 10). *$p < 0.05$, **$p < 0.01$.

sure the levels of inflammatory mediators *IL-6*, *IL-1*β, and Tumor necrosis factor-alpha (*TNF-*α). Minimal infiltration of inflammatory cells and damage was observed in the lung tissue of the control group. The LPS group demonstrated significant infiltration of inflammatory cells and tissue destruction. However, the LPS+TRIM27 group exhibited a reduction in inflammation levels in pulmonary tissue, resembling that of the control group (Fig. 1A). This suggests that TRIM27 treatment can alleviate lung tissue damage. *IL-6*, an important inflammatory mediator, reflects the severity of inflammation. *IL-6* levels were elevated in the LPS group, but decreased in the LPS+TRIM27 group ($p < 0.01$) (Fig. 1B), suggesting that TRIM27 administration can reduce the inflammatory reaction. Similarly, the LPS group exhibited elevated levels of the pro-inflammatory cytokines, *IL-1*β and *TNF-*α. However, in the LPS+TRIM27 cohort, the concentrations of *IL-1*β and *TNF-*α were diminished, nearing the levels observed in the control group ($p < 0.01$) (Fig. 1C,D). This provides additional evidence that TRIM27 administration can suppress the synthesis of pro-inflammatory cytokines.

TRIM27 Induces Autophagy in LPS-Stimulated Mice

The LC3-II/I level indicates autophagy activity, serving as a marker for autophagy. LC3-II/I was comparatively low in the control group but elevated in the LPS group, suggesting that LPS stimulation can trigger autophagy. LC3-II/I was further elevated in the LPS+TRIM27 group, suggesting that the administration of TRIM27 can further en-

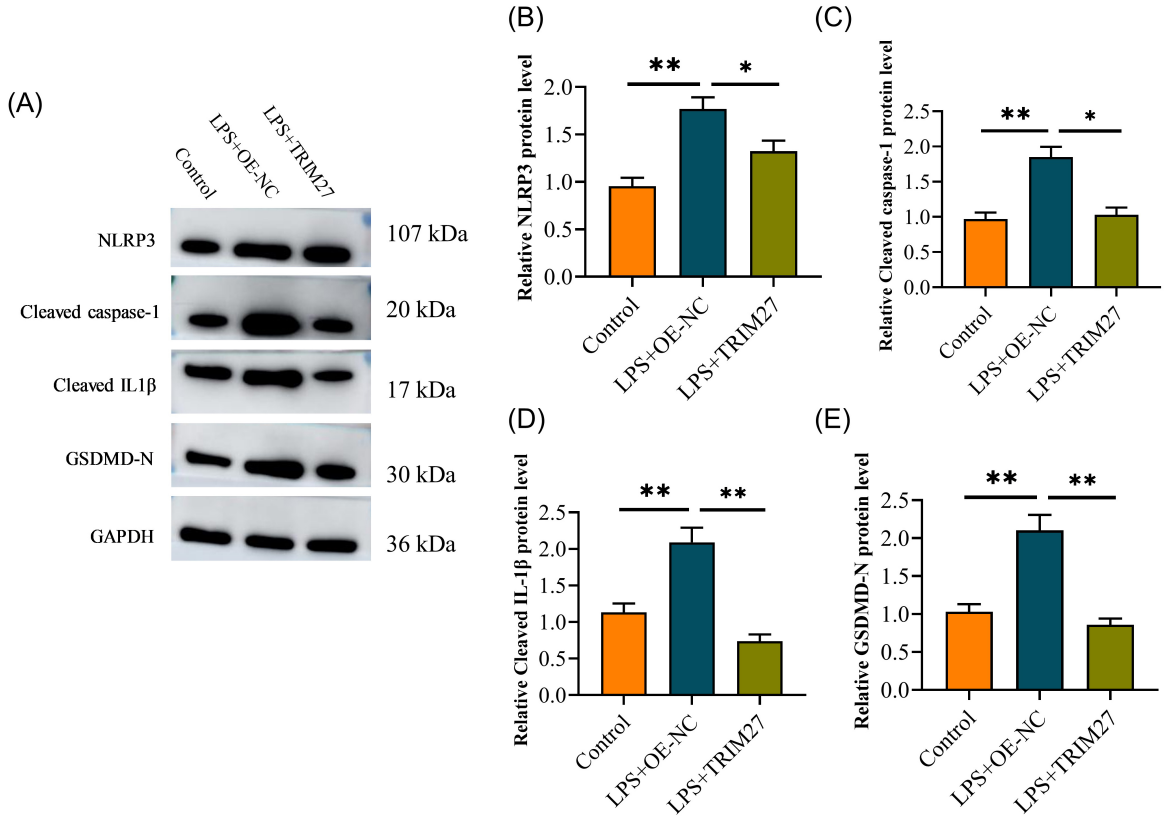

Fig. 3. TRIM27 inhibits cell pyroptosis by inducing autophagy in mouse lung tissues. (A–E) Analysis of NOD-like receptor thermal protein domain associated protein 3 (*NLRP3*), cleaved caspase-1, cleaved IL-1β, and Gasdermin D N-terminal fragment (GSDMD-N) protein expression levels in mouse lung tissues (n = 10). *$p < 0.05$, **$p < 0.01$.

hance autophagy activity ($p < 0.05$) (Fig. 2A,B). p62 exhibited a relatively high level in the control group. In contrast, p62 was decreased in the LPS group and further decreased in the LPS+TRIM27 cohort ($p < 0.05$) (Fig. 2A,C). Beclin-1, a key protein the reflects the initiation of autophagy, exhibited a relatively low level in the control group. However, in the LPS group, its expression increased, suggesting that LPS stimulation could enhance the onset of autophagy ($p < 0.05$). Moreover, in the LPS+TRIM27 group, Beclin-1 expression further increased, suggesting that TRIM27 administration can augment the initiation of autophagy ($p < 0.01$) (Fig. 2A,D). Pulmonary epithelial cells are a part of the respiratory system, and their cellular environment and functions may differ from those of other cell types. TRIM27 potentially induces autophagy in pulmonary epithelial cells.

TRIM27 Suppresses Pyroptosis by Inducing Autophagy

NLRP3, an inflammasome-related protein reflecting the extent of pyroptosis, exhibited a comparatively low level in the control group. However, NLRP3 was increased in the LPS group, suggesting that LPS stimulation can trigger pyroptosis ($p < 0.01$) (Fig. 3A,B). NLRP3 was decreased in the LPS+TRIM27 cohort ($p < 0.05$) (Fig. 3A,B). The activity of pyroptosis can be determined by assessing the level of cleaved caspase-1, an essential protein involved in pyroptosis. Caspase-1 cleavage was comparatively minimal in the control group. However, within the LPS group, cleaved caspase-1 levels were elevated, suggesting that LPS stimulation can induce pyroptosis ($p < 0.01$). Caspase-1 cleavage levels were decreased in the LPS+TRIM27 group ($p < 0.05$) (Fig. 3A,C). The production of cleaved IL-1β is a consequence of pyroptosis, and its quantity indicates the magnitude of pyroptosis. The level of cleaved IL-1β was comparatively low in the control group. However, there was an increase in cleaved IL-1β in the LPS group ($p < 0.01$) (Fig. 3A,D). Cleaved IL-1β was decreased in the LPS+TRIM27 cohort. GSDMD-N, a protein that reflects the extent of pyroptosis, exhibited comparatively low levels in the control group. However, within the LPS cohort, GSDMD-N levels were increased in the LPS cohort, suggesting that LPS stimulation promotes the upregulation of pyroptosis-associated proteins. In contrast, the LPS+TRIM27 group exhibited a decrease in GSDMD-N, suggesting that treatment with TRIM27 can diminish the expression of pyroptosis-associated proteins induced by LPS ($p < 0.01$) (Fig. 3A,E). The experimental findings suggest that autophagy induction through TRIM27 treatment effectively suppresses pyroptosis.

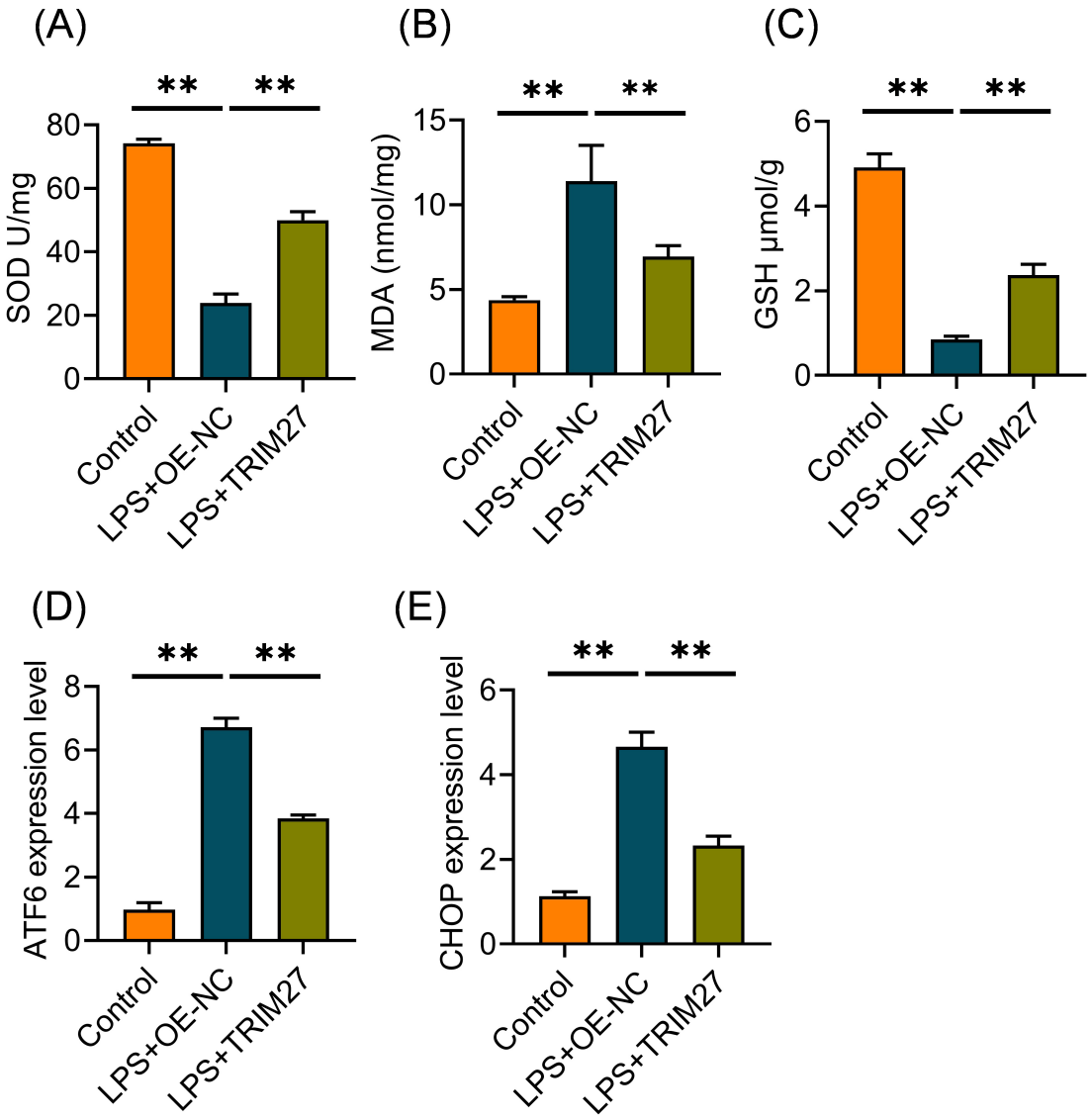

Fig. 4. Induction of protective autophagy by TRIM27 hinders oxidative stress and endoplasmic reticulum stress. (A–C) Levels of superoxide dismutase (SOD) (A), malondialdehyde (MDA) (B), and glutathione (GSH) (C) in lung tissues of mice were detected by enzyme-linked immunosorbent assay (ELISA). (D,E) The mRNA levels of *ATF6* and *CHOP* in the lung tissues of mice were measured by RT-qPCR (n = 10). $^{**}p < 0.01$.

Induction of Protective Autophagy by TRIM27 Hinders Oxidative Stress and Endoplasmic Reticulum Stress

Superoxide dismutase (SOD) is an antioxidant enzyme that reflects the extent of intracellular oxidative stress. The LPS group exhibited a decrease in SOD, suggesting that LPS stimulation can potentially elevate intracellular oxidative stress. TRIM27 administration resulted in increased SOD levels in the LPS+TRIM27 group, suggesting its potential to suppress LPS-induced oxidative stress ($p < 0.01$) (Fig. 4A). The control group exhibited low intracellular oxidative stress, indicated by low levels of malondialdehyde (MDA). However, MDA was increased in the LPS group, suggesting that LPS stimulation can enhance the generation of intracellular oxidative stress compounds. In the LPS+TRIM27 group, MDA levels were decreased, suggesting that TRIM27 treatment can potentially diminish the generation of oxidative stress compounds caused by LPS ($p < 0.05$) (Fig. 4B). The antioxidant glutathione (GSH) exhibited reduced levels in the LPS group but was elevated in the LPS+TRIM27 group, suggesting that treatment with TRIM27 can alleviate LPS-induced oxidative stress ($p < 0.01$) (Fig. 4C). Activating Transcription Factor 6 (*ATF6*) and C/EBP-homologous protein (*CHOP*) are endoplasmic reticulum stress-related proteins, and their levels reflect the extent of intracellular endoplasmic reticulum stress. The LPS group exhibited elevated levels of both *ATF6* and *CHOP*, suggesting that LPS stimulation can enhance intracellular endoplasmic reticulum stress. In contrast, *ATF6* and *CHOP* levels were reduced in the LPS+TRIM27 group,

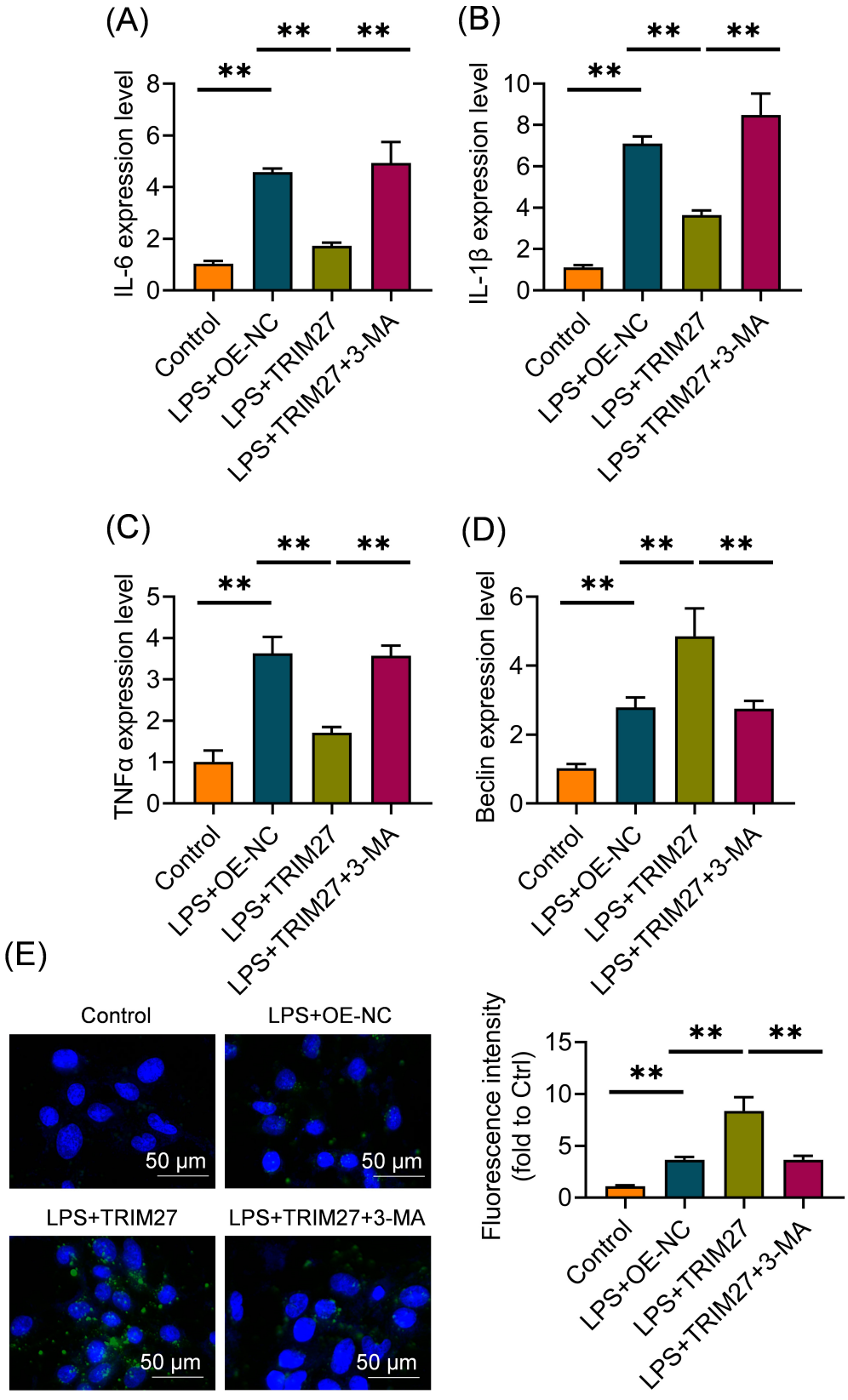

Fig. 5. Autophagy inhibitor reverses the protective effect of TRIM27 on pneumonia. (A–D) The mRNA expression levels of *IL-6* (A), *IL-1β* (B), *TNF-α* (C), and Beclin-1 (D) in mouse lung endothelial cells were detected by RT-qPCR. (E) Results of autophagosome fluorescence staining. Blue represents the cell nuclei stained with Hoechst dye, and green represents the fluorescence labeling of the LC3B antibody (n = 6) (**$p < 0.01$).

suggesting that treatment with TRIM27 can suppress endoplasmic reticulum stress induced by LPS ($p < 0.01$) (Fig. 4D,E).

Autophagy Inhibitor Reverses the Protective Effect of TRIM27 on Pneumonia

Inflammatory responses involve three crucial inflammatory cytokines, namely *IL-6*, *IL-1*β, and *TNF-*α. The levels of these three enzymes were increased in the LPS group ($p < 0.01$) but decreased in the LPS+TRIM27 group ($p < 0.01$), suggesting its potential to alleviate the LPS-induced inflammatory response ($p < 0.01$). However, the LPS+TRIM27+3-MA group exhibited elevated levels of *IL-6*, *IL-1*β, and *TNF-*α, suggesting that the protected effect of TRIM27 on the inflammatory response can be reversed by the autophagy inhibitor 3-MA ($p < 0.01$) (Fig. 5A–C). The Beclin-1 expression level was elevated in the LPS group, suggesting that LPS stimulation can enhance autophagy. The Beclin-1 expression level was further elevated in the LPS+TRIM27 group but decreased in the LPS+TRIM27+3-MA group, suggesting that the autophagy inhibitor 3-MA can counteract the enhancing impact of TRIM27 on autophagy ($p < 0.01$) (Fig. 5D). Autophagosomes are structures formed during the process of autophagy and can be observed through fluorescence staining. The LPS group showed an increase in autophagosome quantity, suggesting that LPS stimulation can potentially enhance autophagy. The LPS+TRIM27 group exhibited further augmentation in autophagosome quantity, suggesting that TRIM27 administration can enhance autophagy. The LPS+TRIM27+3-MA group exhibited a decrease in the number of autophagosomes, suggesting that the autophagy suppressant 3-MA can counteract the enhancing impact of TRIM27 on autophagy (Fig. 5E).

Discussion

Pneumonia is a common respiratory infection that can lead to respiratory distress, lung function failure, and even death in severe cases [24]. Therefore, it is highly important to discover novel therapeutic approaches that can relieve pneumonia-induced inflammation, oxidative stress, and endoplasmic reticulum stress, as this will greatly enhance the outlook for affected patients [25]. During this investigation, TRIM27 demonstrated a safeguarding function in pneumonia through the stimulation of defensive autophagy.

Firstly, we observed that TRIM27 overexpression alleviated lung tissue damage in a lipopolysaccharide (LPS)-induced pneumonia mouse model. Additional tests revealed that TRIM27 triggered autophagy in mice stimulated with LPS, indicating that TRIM27 exerts its protective benefits through the regulation of the autophagy pathway. Autophagy, a process of self-degradation within cells, helps maintain cellular balance by engulfing and breaking down damaged organelles and proteins, as well as eliminating harmful substances and metabolic byproducts [26]. In pneumonia, autophagy can be controlled, thereby impacting the disease's advancement and intensity [27]. The findings of this study indicate that the activation of TRIM27 boosts autophagy, consequently improving the lung tissue's capacity for self-repair, reducing cellular damage, and alleviating inflammation caused by pneumonia.

Additional findings from this study indicate that TRIM27 suppresses both oxidative and endoplasmic reticulum stress through the stimulation of defensive autophagy. Oxidative stress is the result of an imbalance in the cellular redox equilibrium, causing an overproduction of reactive oxygen species [28]. This leads to cell damage, triggering inflammatory reactions. Endoplasmic reticulum stress is the result of endoplasmic reticulum dysfunction that causes irregular protein production and folding, ultimately inducing cellular stress and activating inflammatory reactions [29]. The results of our experiment show that the introduction of TRIM27 reduces both oxidative and endoplasmic reticulum stress, thus mitigating cellular damage and inflammatory reactions triggered by pneumonia. These findings imply that TRIM27 can uphold cellular balance and relieve cellular stress and inflammation resulting from pneumonia by controlling the autophagy pathway.

Furthermore, our experimental findings demonstrated that the autophagy suppressant 3-MA can counteract the safeguarding impact of TRIM27 on pneumonia, which further confirms the importance of autophagy regulation as a mechanism of TRIM27's protective effect. The initiation and progression of autophagy are affected by 3-MA, a frequently employed inhibitor of autophagy, which inhibits its occurrence and impacts. Our findings suggest that autophagy inhibition reverses the protective impact of TRIM27 on pneumonia, thereby highlighting the importance of autophagy.

The role of TRIM27 in pneumonia is showcased in this study. Pneumonia-induced cellular damage and inflammatory responses are alleviated by TRIM27 through regulation of the autophagy pathway. The discovery offers fresh perspectives on comprehending the processes involved in pneumonia manifestation and pinpointing novel targets for treatment. Furthermore, this research also holds significance for the management of various inflammatory conditions, including infectious diseases, autoimmune diseases, and tumors, which are commonly associated with inflammation. The defensive autophagy induced by TRIM27 may have potential applications in the treatment of other inflammatory conditions, presenting new opportunities for innovative therapeutic strategies.

Conclusion

TRIM27 mitigates the effects of pneumonia by inducing defensive autophagy, thereby relieving inflammation, oxidative stress, and endoplasmic reticulum stress. Enhanc-

ing autophagic activity through TRIM27 induction helps maintain cellular homeostasis, and alleviate cellular damage and inflammatory responses resulting from pneumonia. However, additional investigation is required to examine the underlying mechanisms of TRIM27 and autophagy.

Availability of Data and Materials

The datasets used or analyzed during the current study are available from the corresponding author on reasonable request.

Author Contributions

YP and HW contributed to the study concept and design. HW, QX, and TM contributed to the acquisition of data. YP performed the statistical analysis. HW was involved in the interpretation of the data. All authors contributed to editorial changes in the manuscript. All authors read and approved the final manuscript. All authors have participated sufficiently in the work and agreed to be accountable for all aspects of the work.

Ethics Approval and Consent to Participate

All procedures were approved by the Animal Ethics Committee of Ningbo University (NO.11679).

Acknowledgment

Not applicable.

Funding

This research received no external funding.

Conflict of Interest

The authors declare no conflict of interest.

References

[1] Hespanhol V, Bárbara C. Pneumonia mortality, comorbidities matter? Pulmonology. 2020; 26: 123–129.

[2] Torres A, Cilloniz C, Niederman MS, Menéndez R, Chalmers JD, Wunderink RG, *et al*. Pneumonia. Nature Reviews. Disease Primers. 2021; 7: 25.

[3] Kumar V. Pulmonary Innate Immune Response Determines the Outcome of Inflammation During Pneumonia and Sepsis-Associated Acute Lung Injury. Frontiers in Immunology. 2020; 11: 1722.

[4] Stevens J, Steinmeyer S, Bonfield M, Peterson L, Wang T, Gray J, *et al*. The balance between protective and pathogenic immune responses to pneumonia in the neonatal lung is enforced by gut microbiota. Science Translational Medicine. 2022; 14: eabl3981.

[5] Zhang S, Li L, Shen A, Chen Y, Qi Z. Rational Use of Tocilizumab in the Treatment of Novel Coronavirus Pneumonia. Clinical Drug Investigation. 2020; 40: 511–518.

[6] Zaragoza R, Vidal-Cortés P, Aguilar G, Borges M, Diaz E, Ferrer R, *et al*. Update of the treatment of nosocomial pneumonia in the ICU. Critical Care (London, England). 2020; 24: 383.

[7] Ichimiya T, Yamakawa T, Hirano T, Yokoyama Y, Hayashi Y, Hirayama D, *et al*. Autophagy and Autophagy-Related Diseases: A Review. International Journal of Molecular Sciences. 2020; 21: 8974.

[8] Cao W, Li J, Yang K, Cao D. An overview of autophagy: Mechanism, regulation and research progress. Bulletin du Cancer. 2021; 108: 304–322.

[9] Lamark T, Johansen T. Mechanisms of Selective Autophagy. Annual Review of Cell and Developmental Biology. 2021; 37: 143–169.

[10] Wollert T. Autophagy. Current Biology: CB. 2019; 29: R671–R677.

[11] Cao X, Wan H, Wan H. Urolithin A induces protective autophagy to alleviate inflammation, oxidative stress, and endoplasmic reticulum stress in pediatric pneumonia. Allergologia et Immunopathologia. 2022; 50: 147–153.

[12] Wang W, Mao Y, Zhu Y. Research progress of autophagy in viral pneumonia. Chinese Journal of Clinical Pharmacology and Therapeutics. 2020; 25: 1315.

[13] Deretic V. Autophagy in inflammation, infection, and immunometabolism. Immunity. 2021; 54: 437–453.

[14] Wang G, Fu Y, Ma K, Liu J, Liu X. NOD2 regulates microglial inflammation through the TAK1-NF-κB pathway and autophagy activation in murine pneumococcal meningitis. Brain Research Bulletin. 2020; 158: 20–30.

[15] Ying Y, Sun CB, Zhang SQ, Chen BJ, Yu JZ, Liu FY, *et al*. Induction of autophagy via the TLR4/NF-κB signaling pathway by astragaloside IV contributes to the amelioration of inflammation in RAW264.7 cells. Biomedicine & Pharmacotherapy = Biomedecine & Pharmacotherapie. 2021; 137: 111271.

[16] Popper HH, Stacher-Priehse E, Brcic L, Eidsenhammer S, Gallob F, Rampp F, *et al*. Autophagy and senescence are activated mechanisms in idiopathic or autoimmunity caused usual interstitial pneumonia. European Respiratory Journal. 2019; 54: PA5379.

[17] Yu C, Rao D, Wang T, Song J, Zhang L, Huang W. Emerging roles of TRIM27 in cancer and other human diseases. Frontiers in Cell and Developmental Biology. 2022; 10: 1004429.

[18] Garcia-Garcia J, Berge AKM, Overå KS, Larsen KB, Bhujabal Z, Brech A, *et al*. TRIM27 is an autophagy substrate facilitating mitochondria clustering and mitophagy via phosphorylated TBK1. The FEBS Journal. 2023; 290: 1096–1116.

[19] Wang X, Zhang H, Shao Z, Zhuang W, Sui C, Liu F, *et al*. TRIM31 facilitates K27-linked polyubiquitination of SYK to regulate antifungal immunity. Signal Transduction and Targeted Therapy. 2021; 6: 298.

[20] Wang S, Lu B, Liu J, Gu Y. TRIM27 suppresses inflammation injuries in pediatric pneumonia by targeting TLR4/NF-κB signaling pathway. Allergologia et Immunopathologia. 2022; 50: 33–39.

[21] Liu S, Yao S, Yang H, Liu S, Wang Y. Autophagy: Regulator of cell death. Cell Death & Disease. 2023; 14: 648.

[22] Nikouee A, Kim M, Ding X, Sun Y, Zang QS. Beclin-1-Dependent Autophagy Improves Outcomes of Pneumonia-Induced Sepsis. Frontiers in Cellular and Infection Microbiology. 2021; 11: 706637.

[23] Zhang Y, Xu S, Li K, Li X, Yin H, Li S, *et al*. TBBPA induced ROS overproduction promotes apoptosis and inflammation by inhibiting autophagy in mice lung. Ecotoxicology and Environmental Safety. 2023; 252: 114607.

[24] Pernica JM, Harman S, Kam AJ, Carciumaru R, Vanniyasingam T, Crawford T, *et al*. Short-Course Antimicrobial Therapy for Pediatric Community-Acquired Pneumonia: The SAFER Randomized Clinical Trial. JAMA Pediatrics. 2021; 175: 475–482.

[25] Arun Prakash J, Asswin CR, Ravi V, Sowmya V, Soman KP. Pediatric pneumonia diagnosis using stacked ensemble learning on multi-model deep CNN architectures. Multimedia Tools and Applications. 2023; 82: 21311–21351.

[26] Dong Y, Jin C, Ding Z, Zhu Y, He Q, Zhang X, *et al*. TLR4 regulates ROS and autophagy to control neutrophil extracellular traps formation against Streptococcus pneumoniae in acute otitis media. Pediatric Research. 2021; 89: 785–794.

[27] Zhang X, Ding M, Zhu P, Huang H, Zhuang Q, Shen J, *et al*. New Insights into the Nrf-2/HO-1 Signaling Axis and Its Application in Pediatric Respiratory Diseases. Oxidative Medicine and Cellular Longevity. 2019; 2019: 3214196.

[28] Jakubczyk K, Dec K, Kałduńska J, Kawczuga D, Kochman J, Janda K. Reactive oxygen species - sources, functions, oxidative damage. Polski Merkuriusz Lekarski: Organ Polskiego Towarzystwa Lekarskiego. 2020; 48: 124–127.

[29] Liu X, Hussain R, Mehmood K, Tang Z, Zhang H, Li Y. Mitochondrial-Endoplasmic Reticulum Communication-Mediated Oxidative Stress and Autophagy. BioMed Research International. 2022; 2022: 6459585.